

Supporting Information

Enhanced Antimicrobial Treatment by a Clay-Based Drug Nanocarrier Conjugated to a Guanidine-Rich Cell Penetrating Peptide

Mohammad Reza Khodabakhshi, Mohammad Hadi Baghersad*

Applied Biotechnology Research Center, Baqiyatallah University of Medical Sciences

*Corresponding author. E-mail address: Hadibaghersad@bmsu.ac.ir (M.H. Baghersad).

Table of content

Content	Page
Table S1. The chemicals used in the project.	S2
Table S2. The instruments used in the project.	S3
Figure S1. The LC-MS result of the synthesis peptide sequence.	S4
Figure S2. EDX spectra and quantitative tables of the raw materials and products.	S5
Figure S3. DLS curves of HNTs.	S6
Estimation of drug content	S7
Figure S4. OD ₆₀₀ experiment: growth inhibition effects of individual VCM and OFX, and nanocargoes on 3T3 fibroblast human normal cells.	S8
Figure S5. Disk counter experiment: digital photos of the dishes including <i>S. aureus</i> bacteria and VCM@Fe ₃ O ₄ /HNT-C(WR) ₃ nanocargo in LB Broth medium, over 24 h incubation.	S9
Figure S6. DLS spectrum of the dispersed VCM@Fe ₃ O ₄ /HNT-C(WR) ₃ nanocargoes in HAS (25%) in the simulated circulatory system, after 15 minutes.	S10
Figure S7. DLS spectrum of the dispersed VCM@Fe ₃ O ₄ /HNT-C(WR) ₃ nanocargoes in HAS (25%) in the simulated circulatory system, after 30 minutes.	S11
Figure S8. DLS spectrum of the dispersed VCM@Fe ₃ O ₄ /HNT-C(WR) ₃ nanocargoes in HAS (25%) in the simulated circulatory system, after 60 minutes.	S12

Table S1. The used chemicals in this project.

Material	Brand & Purity
Solvents	Merck
Halloysite nanoclay	Sigma-Aldrich
FeCl ₂ .4H ₂ O	Sigma-Aldrich, ≥98.0%
FeCl ₃ .6H ₂ O	Sigma-Aldrich, ≥97.0%
(3-Mercaptopropyl)trimethoxysilane	Sigma-Aldrich, 95.0%
Vancomycin	Sigma-Aldrich
Ofloxacin	Sigma-Aldrich
2-Chlorotriyl chloride (CTC) resin	Sigma-Aldrich
Hydrogen peroxide (30 wt%)	Merck
TBTU	Sigma-Aldrich
N,N-Diisopropylethylamine	Sigma-Aldrich, ≥99.0%
Piperidine	Sigma-Aldrich, ≥99.0%
Trifluoroacetic acid	Sigma-Aldrich, ≥99.0%
Triethyl silane	Sigma-Aldrich, 98%
Fmoc-Trp(Trt)-OH	Sigma-Aldrich, ≥98.0%
Fmoc-Arg(Pbf)-OH	Sigma-Aldrich, ≥98.0%
Fmoc-Cys(Trt)-OH	Sigma-Aldrich, ≥98.0%
Bacteria cell lines	S. aureus-ATCC 12600 and E. coli-ATCC 9637
3T3 fibroblast cells	Iranian Biological Resource Center
HAS (25%)	Octapharma (Vienna, Austria)
Crystal violet (tris(4-(dimethylamino)phenyl)methylum chloride)	Merck, ≥90.0%
Dulbecco's modified Eagle's medium (DMEM)	Sigma-Aldrich

Table S2. The used equipment in this project.

Equipment	Brand
Ball-mill	Amin Asia Fanavar Pars Co. (IRAN)
Furnace	Carrier Furnace Units
Autoclave for sterilization	Reyhan Teb, 2KW-220v
Thermometer	Fluke (572-2 infrared)
Ultrasound probe	Hielscher (UP100H)
Ultrasound bath	Steelco US 80
Centrifuge	Beckman Coulter GmbH
Vacuum oven	IQS Directory
Oven	Genlab Ltd
Vortex mixer	OHAUS Europe GmbH
Freeze drier	KASSEL Machinery (Zhejiang) Co.,Ltd
Rotary evaporator	Heidolph Instruments GmbH & Co. KG
Vacuum pump	Amila Automation Technology Suzhou Co,Ltd manufacturer
FTIR spectroscopy	Shimadzu FTIR-8400S
EDX spectroscopy	VEGA-TESCAN-XMU
FESEM	Hitachi S-5200
TEM	Philips CM200
TGA	TGA-Bahr-STA 504, under argon
DLS	Horiba (SZ-100)
VSM	Meghnatis Kavir Kashan Co., Kashan, Iran
XRD	DRON-8 X-ray diffractometer
UV-DRS	Shimadzu-UV-2550/220v
UV-vis spectroscopy	Beckman DU640
LC-MS	Agilent 6410 Triple Quadrupole, Agilent 1200 series Santa Clara, CA, USA
Confocal microscopy	Zeiss LMS 700
Incubator	Sh, Noor Sanat Ferdos

LC-MS ESI

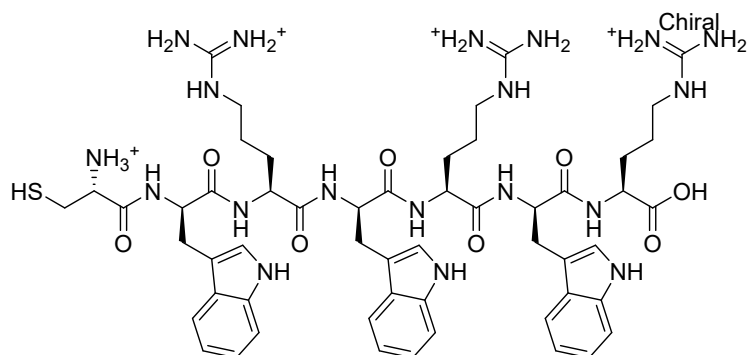
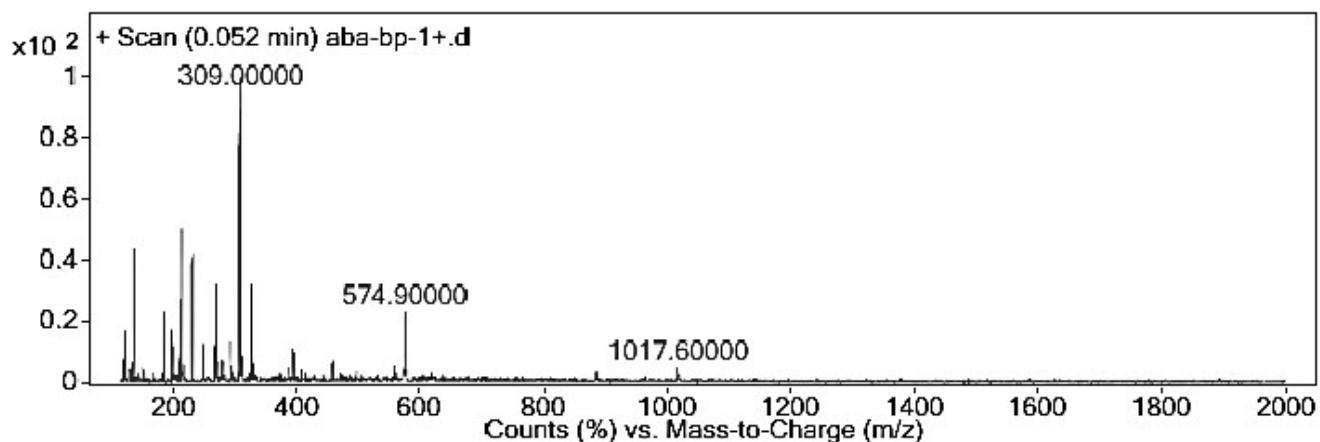


Figure S1. The LC-MS result of the synthesized C(WR)₃ peptide sequence.

Interpretation of the LC-MS result

Since, the ESI technique in positive state (+scan) has been used, two indicative signals are expected to be seen; $[M+1]^+$ and $[M+2H]^{2+}/2$. As is observed in the LC-MS spectrum, a signal at m/z 574.9 has appeared that is attributed to $[M+2H]^{2+}/2$ signal, confirming successful formation of the C(WR)₃ peptide sequence. Considering the MW of the C(WR)₃ sequence (1147.59 g/mol), the signal of $[M+1]^+$ has not been appeared that is a common behavior for the heavy chains. In fact, this is a probable happening for the heavy chains to break down to the smaller chains upon exposure to the ionizing agent. As is observed in the spectrum, a signal at m/z 309.0 has emerged, which can be ascribed to the broken small pieces.

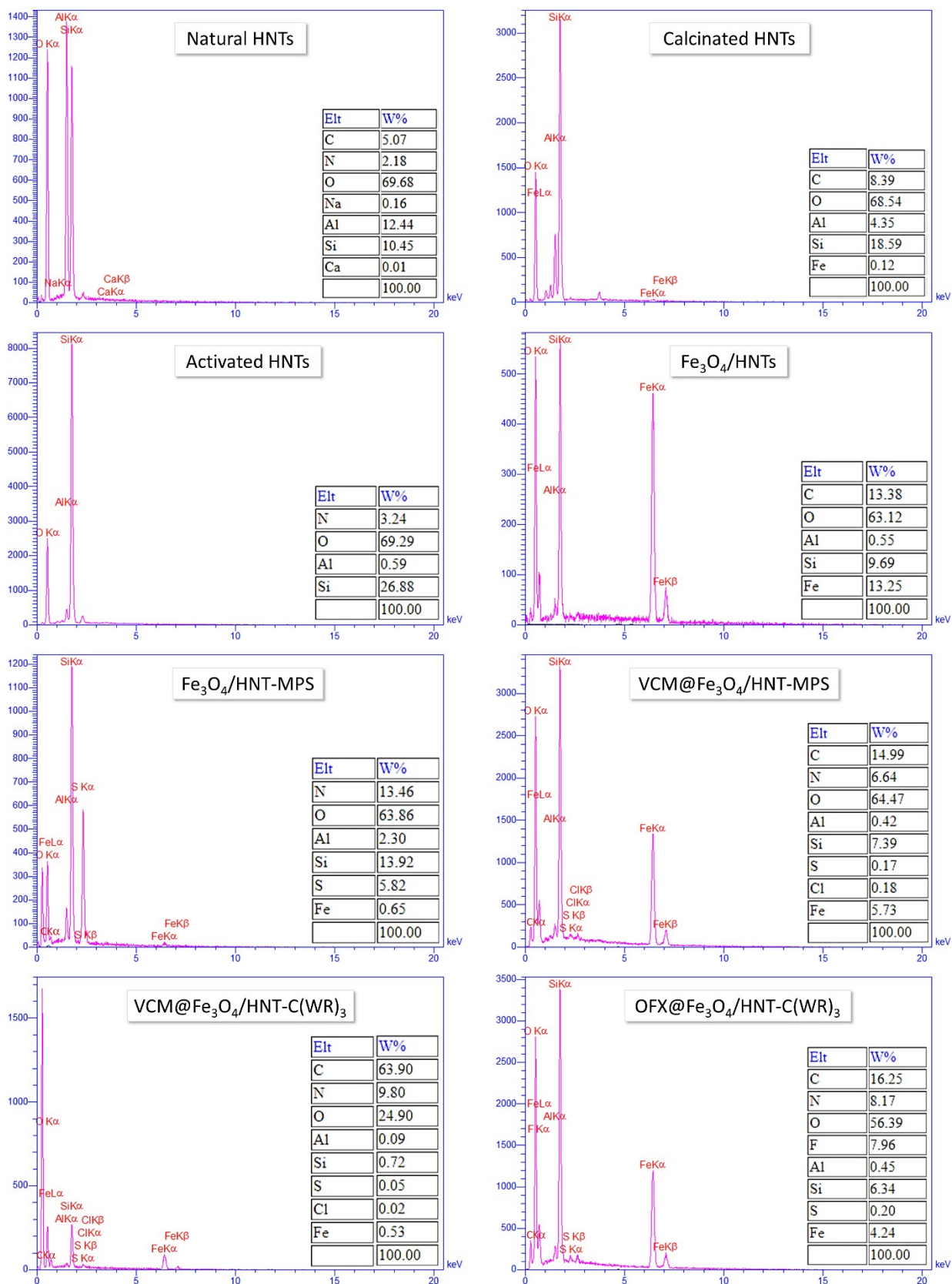


Figure S2. EDX spectra and quantitative tables of the raw materials and products.

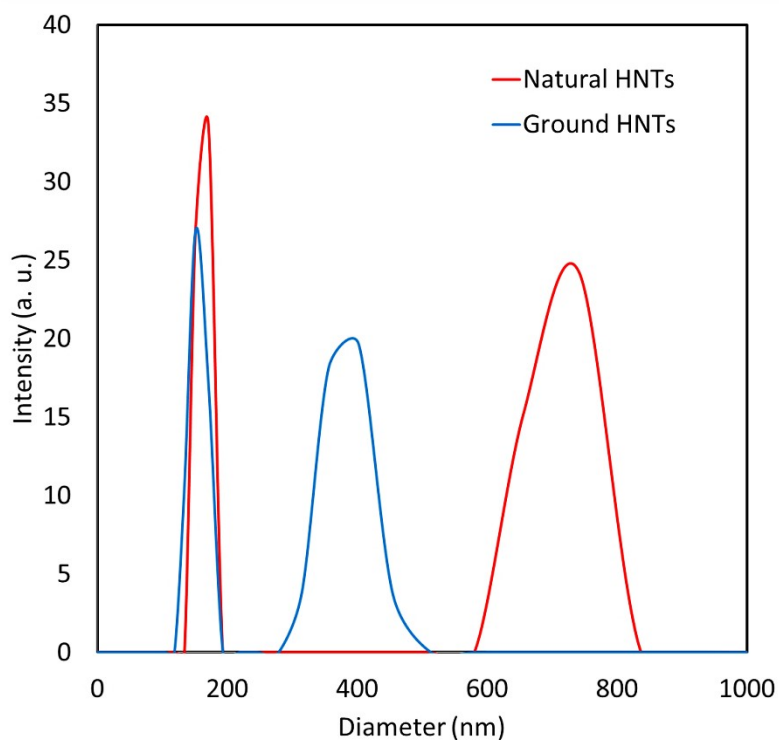


Figure S3. DLS curves of HNTs: the peaks with larger PDI values origin from large pieces of HNTs, and confirm well breakage into smaller pieces. As is observed, the average size of the small pieces of HNTs in the dispersed state is ca. 180 nm, and has not changed during the grinding stage.

Estimation of drug content

For VCM: After filtration and dilution of the sample (1 to 25 mL), the UV-vis absorbance was investigated, as below:

$$A = 0.138 = y$$

From the line equation of the calibration curve;

$$X \text{ (ppm)} = y \text{ (a. u.)} - 0.0305 / 0.0135$$

$$\Rightarrow X = C \text{ (ppm)} = 7.96 \sim 8.0 \text{ ppm (concentration of VCM after dilution)}$$

$$\text{Concentration of VCM before dilution} = 8.0 \times 25 = 200 \text{ ppm} = 0.2 \text{ mg/mL}$$

$$\text{Concentration of VCM in the initial sample} = 5.0 \text{ mg}/25 \text{ mL DMSO}$$

Since, 50 mg of VCM@Fe₃O₄/HNT-C(WR)₃ was dispersed in 25 mL of DMSO, the drug content can be estimated as below:

$$\text{Drug content of VCM@Fe}_3\text{O}_4\text{/HNT-C(WR)}_3 = 5.0 / 50 \times 100 = \mathbf{10 \text{ wt\%}}$$

The same method was passed for OFX

$$A = 0.680$$

$$\text{From line equation: } X \text{ (ppm)} = y \text{ (a. u.)} - 0.202 / 0.0498$$

$$C \text{ (ppm)} = 9.59 \sim 9.6 \text{ ppm (after dilution)}$$

$$9.6 \times 25 = 240 \text{ ppm} = 0.24 \text{ mg/mL (before dilution)}$$

$$0.24 \times 25 = 6.0 \text{ mg}/25 \text{ mL DMSO}$$

$$\text{Drug content of OFX@Fe}_3\text{O}_4\text{/HNT-C(WR)}_3 = 6.0 / 50 \times 100 = \mathbf{12 \text{ wt\%}}$$

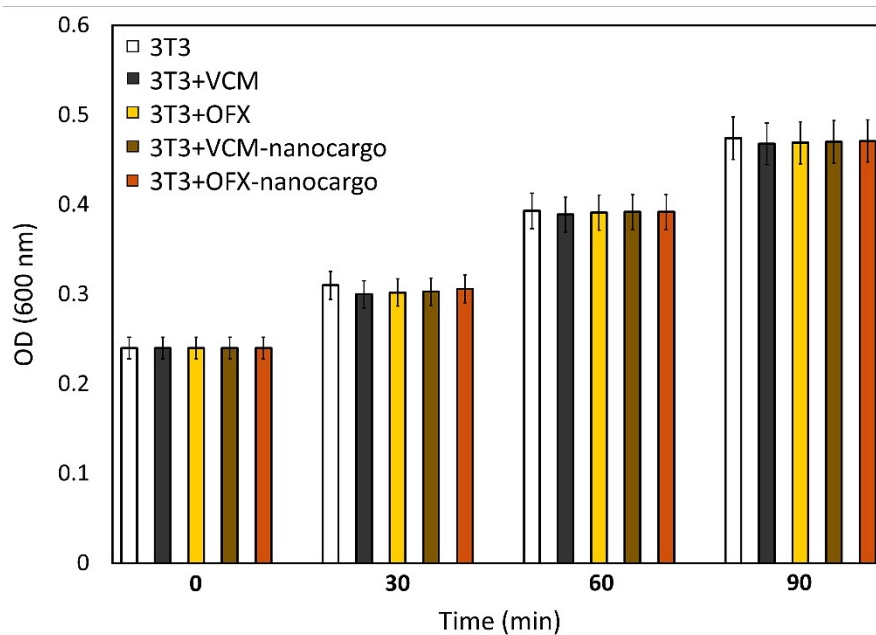


Figure S4. OD_{600} experiment: growth inhibition effects of individual VCM and OFX, and VCM@Fe₃O₄/HNT-C(WR)₃ and OFX@Fe₃O₄/HNT-C(WR)₃ nanocargoes on 3T3 fibroblast human normal cells. All samples have been prepared and subjected to the cells in the same concentration of 50 µg/mL (in DMEM). Ultrasonication in a bath with 50 KHz frequency and 100 W L⁻¹ power density (2 minutes, at room temperature) was performed on the heterogeneous samples to make fine dispersions. The error bars show relative error (%) for three samples of each condition (n = 3).

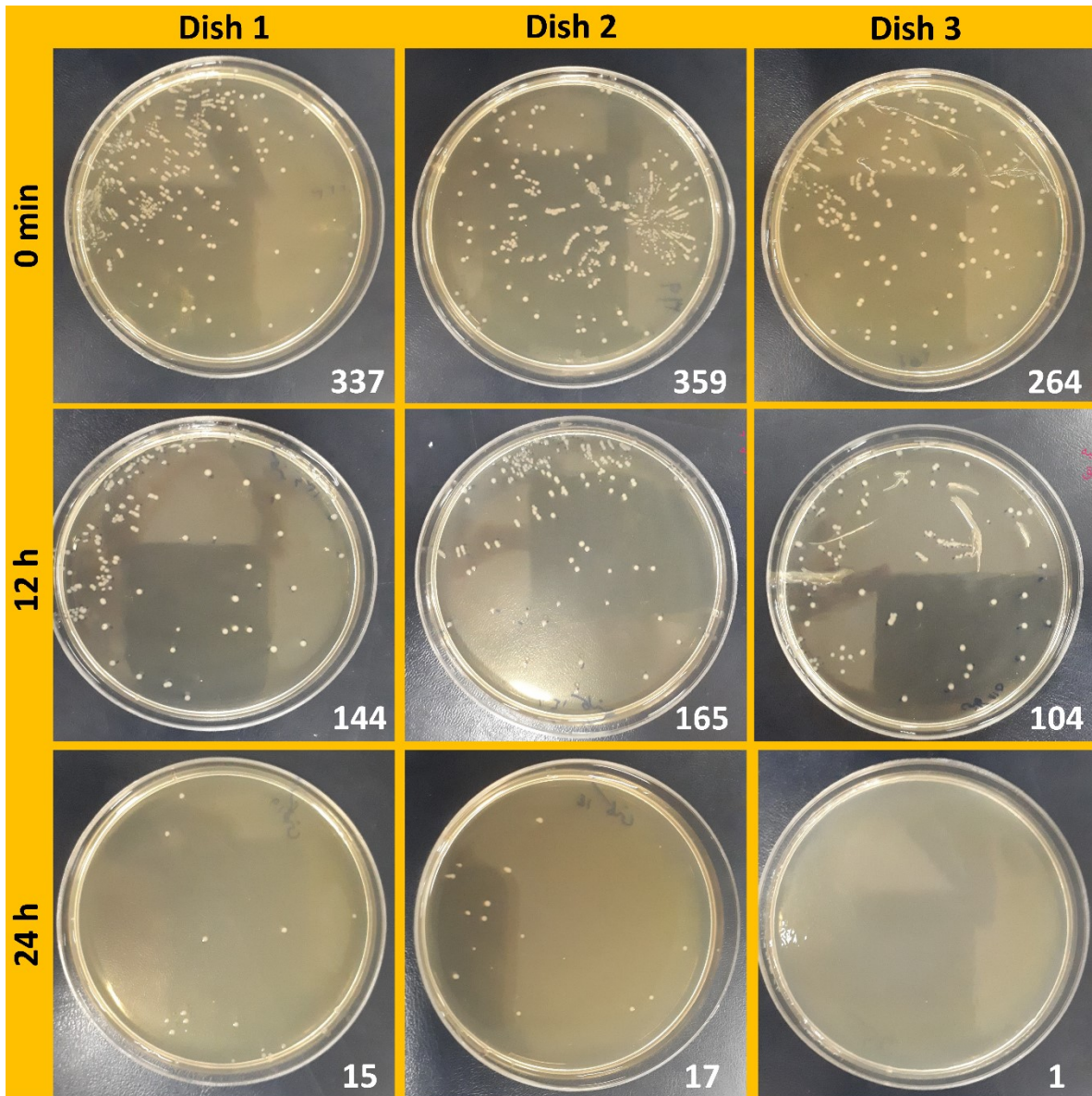


Figure S5. *Disk counter experiment:* digital photos of the dishes including *S. aureus* bacteria and VCM@Fe₃O₄/HNT-C(WR)₃ nanocargo in LB Broth medium, over 24 h incubation.

Cumulant Operations

Z-Average

: 513.3 nm

PI

: 0.859

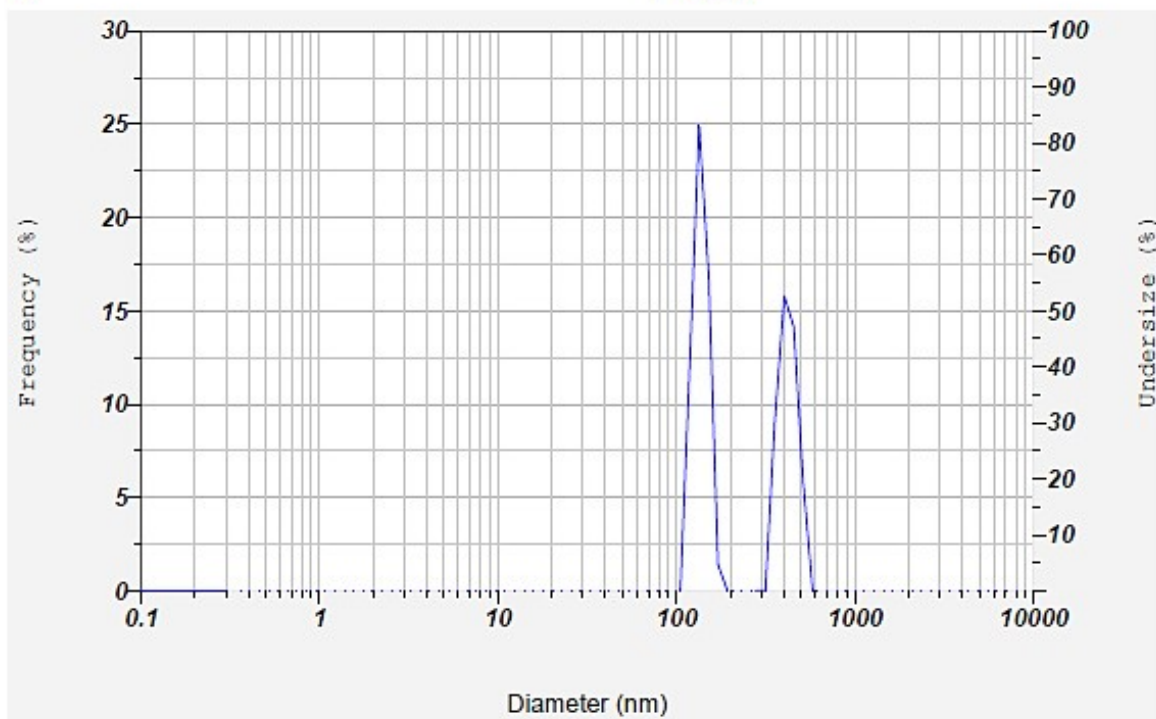


Figure S6. DLS spectrum of the dispersed VCM@Fe₃O₄/HNT-C(WR)₃ nanocargoes in HAS (25%) in the simulated circulatory system, after 15 minutes.

Cumulant Operations

Z-Average

: 873.2 nm

PI

: 0.505

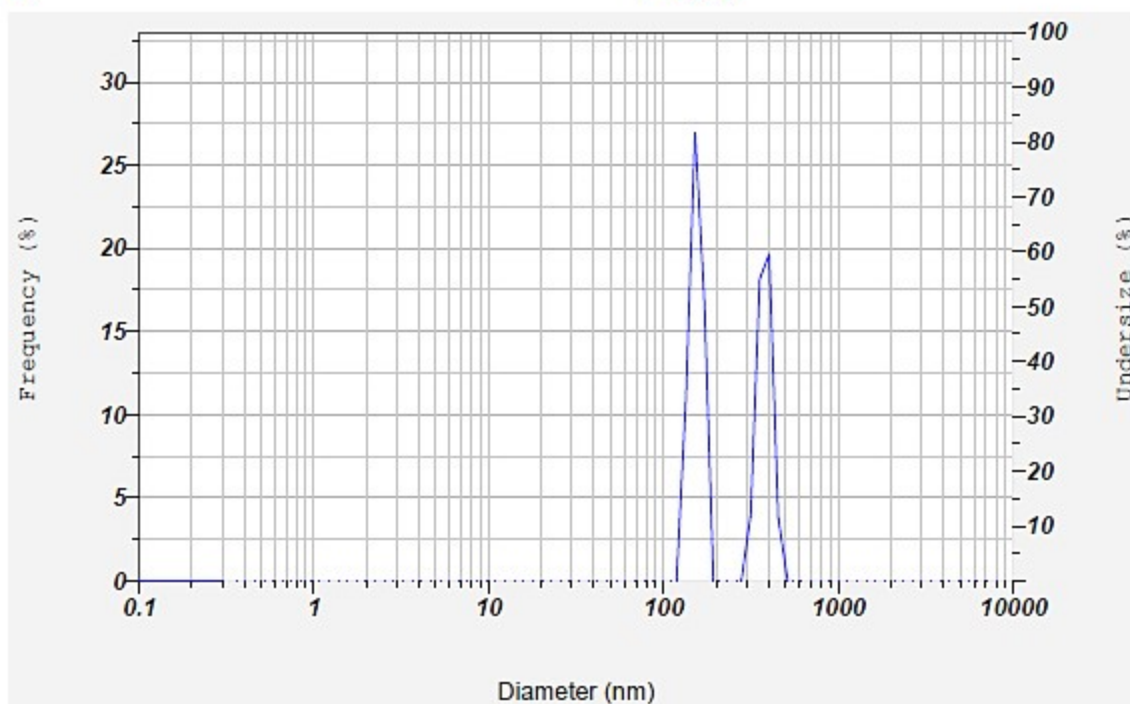


Figure S7. DLS spectrum of the dispersed VCM@Fe₃O₄/HNT-C(WR)₃ nanocargoes in HAS (25%) in the simulated circulatory system, after 30 minutes.

Cumulant Operations

Z-Average

: 1355.1 nm

PI

: 0.720

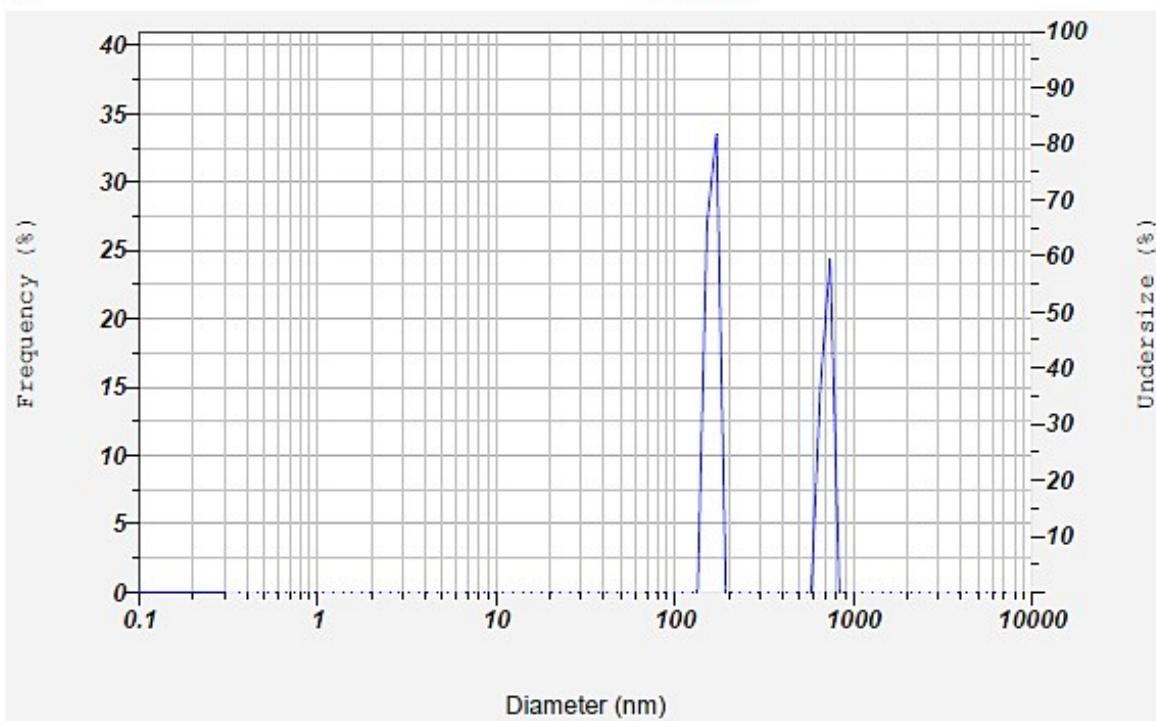


Figure S8. DLS spectrum of the dispersed VCM@Fe₃O₄/HNT-C(WR)₃ nanocargoes in HAS (25%) in the simulated circulatory system, after 60 minutes.